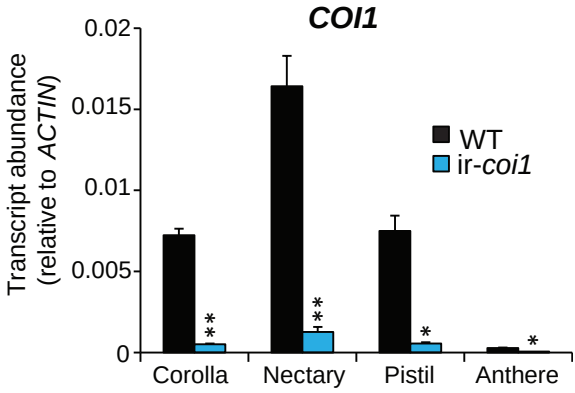

Supplemental Figure 1. *COI1* transcript levels are silenced to similar levels in all floral tissues of ir-*coi1* plants. Transcript abundance (relative to gene expression of *ACTIN*) of *COI1* in individual floral tissues of WT and ir-*coi1* plants on the day before anthesis (mean + SE, n = 3, each replicate was obtained from 20+ pooled tissues of 3 plants). Asterisks represent significant differences between the same floral tissue of WT and ir-*coi1* (unpaired t-test; *, p <0.05; **, p <0.001).

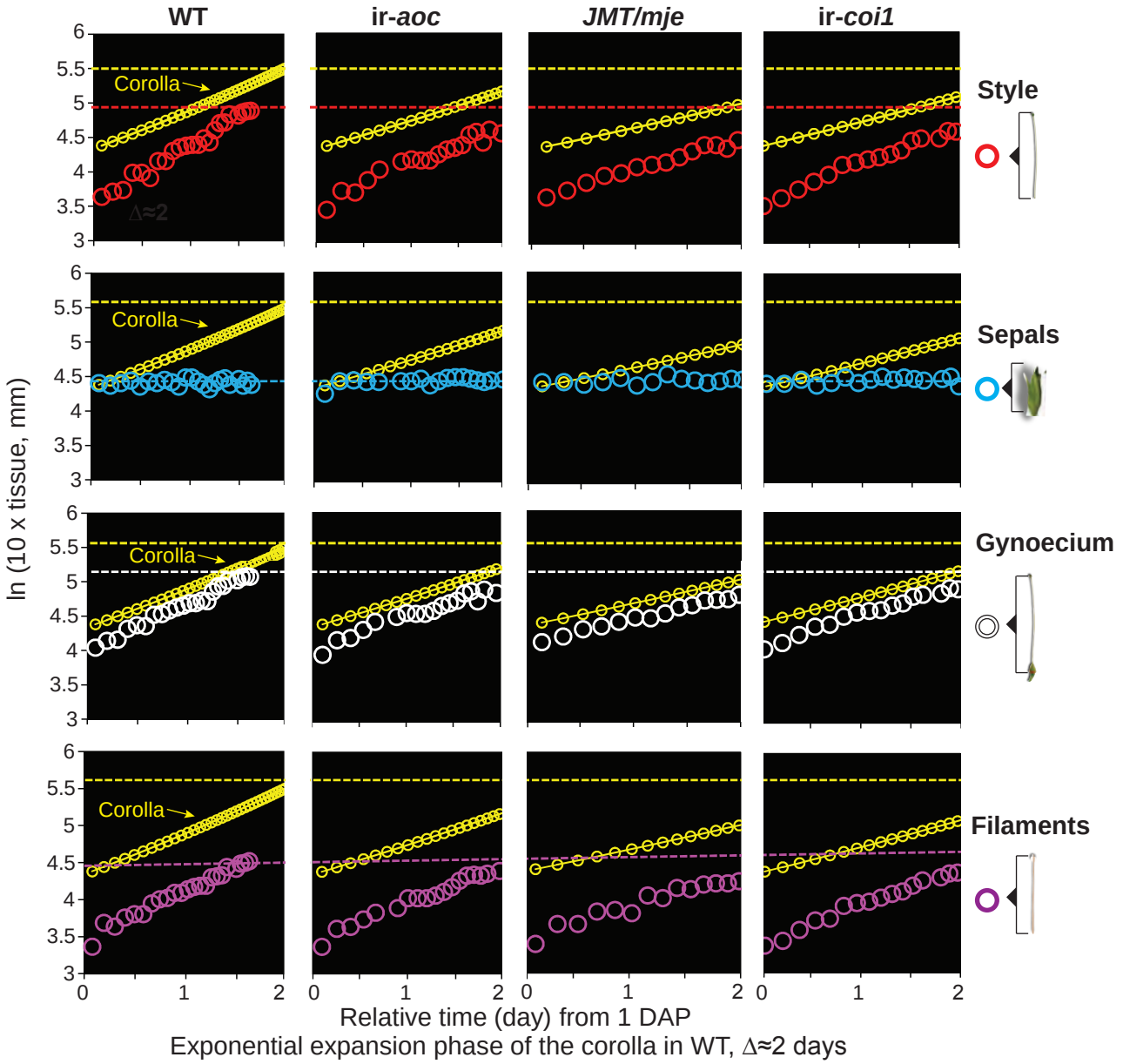

Supplemental Figure 2. The growth rate of different flower organs is altered in JAs biosynthesis/perception-deficient transgenic lines during rapid corolla elongation. Best fits for exponential regressions obtained from ln-transformed corolla size (mm) values were used to calculate relative time from corolla protrusion (expressed in DAP, days after the corolla first protruded the sepals) during the duration of the WT corolla exponential elongation phase (2 DAP) in the different genetic backgrounds. Ln-transformed 10 x tissue size (mm) values measured from individual flowers of the different genotypes were plotted against this relative time difference to model the growth of these tissues during the phase of rapid growth in WT flowers. Except for sepals, the different plots highlight major decreases in the growth rate and outcome sizes (scaled down by ln-transformation) at the end of the measurement time window for the different organs of the transgenic lines compared to those of WT plants. Dashed lines indicate WT floral organ length of corolla (yellow), style (red), sepals (blue), gynoecium (white) and filaments (purple) at the end of WT exponential elongation phase (2 DAP).

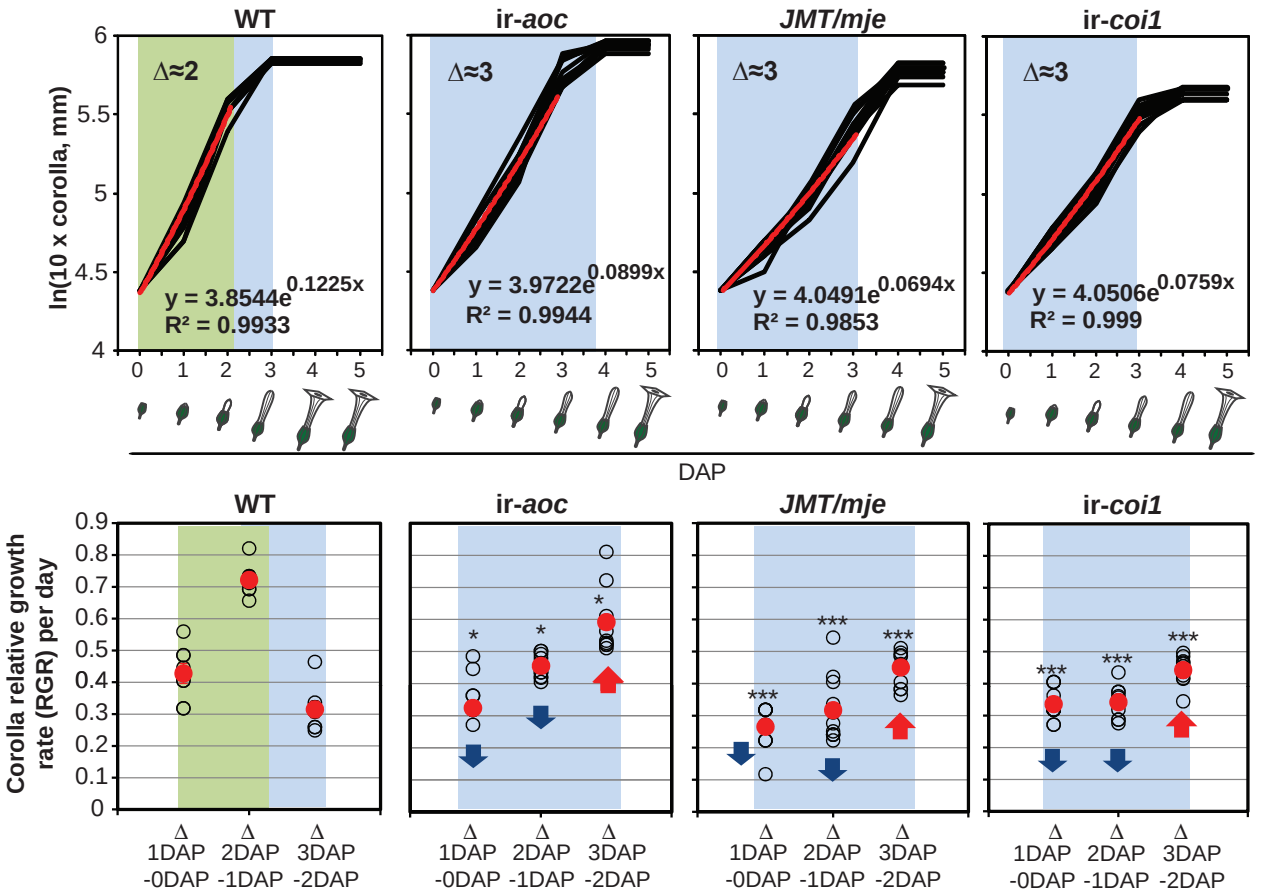

Supplemental Figure 3. Relative growth rate calculations indicate phase-specific effects of JAs signaling deficiency on corolla growth. Corolla length was recorded after dissection from independent flowers collected during the corolla exponential expansion phase of WT flowers (first two days after corolla protrusion, 1 DAP to 3 DAP, range of WT corolla sizes: 8 to 25.3 mm). The duration (Δ in upper panel) of the corolla exponential phase is approximately one day longer in all JAs biosynthesis/perception transgenic plants tested. Best fits for exponential regressions calculated for ln-transformed corolla size (mm) values for each genotype are presented. Corollas' relative growth rates (RGR) per day were calculated according to (Hill and Malmberg, 1991). Asterisks represent significant differences between RGR of WT and transgenic lines at the same DAP (unpaired t-test; *, p <0.05; *** p <0.0001).

Supplemental Data. Stitz et al. Plant Cell (2014) 10.1105/tpc.114.128165

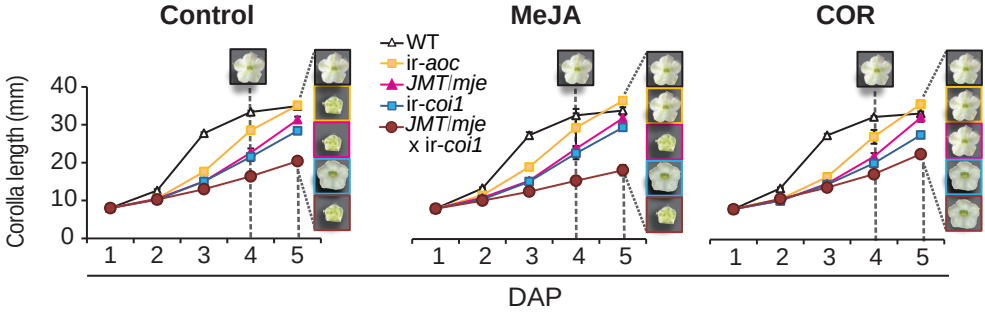

Supplemental Figure 4. Delayed maturation of ir-aoc, JMT/mje, and ir-coi1 cannot be recovered by MeJA or coronatine (COR) treatment. Mean (± SD, n = 5) increase in corolla length in intervals of 1 day from 1 DAP (the day after the corolla protruded the sepals) until anthesis. Plants were treated prior measurements every other day for 10 days with 100 µM MeJA, 1 µM COR or a control solution. Insets indicate days of corolla limb opening.

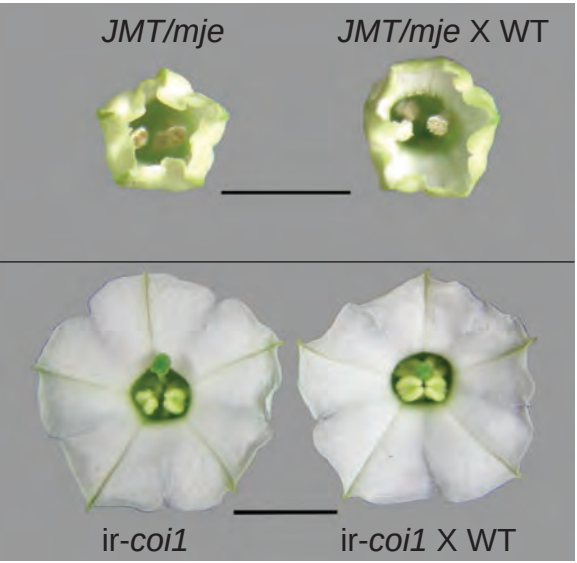

Supplemental Figure 5. Crosses between WT and ir-*coi1* and *JMT*/*mje* plants exhibit corolla phenotypes of their transgenic parents. Flowers of heterozygous plants derived by crosses between WT and *JMT*/*mje* show the characteristic defective limb opening for JAs deficient plants. The back cross with ir-*coi1* shows complete limb opening and the typically un-dehiscing anthers of homozygous ir-*coi1*. Scale bar, 5 mm.

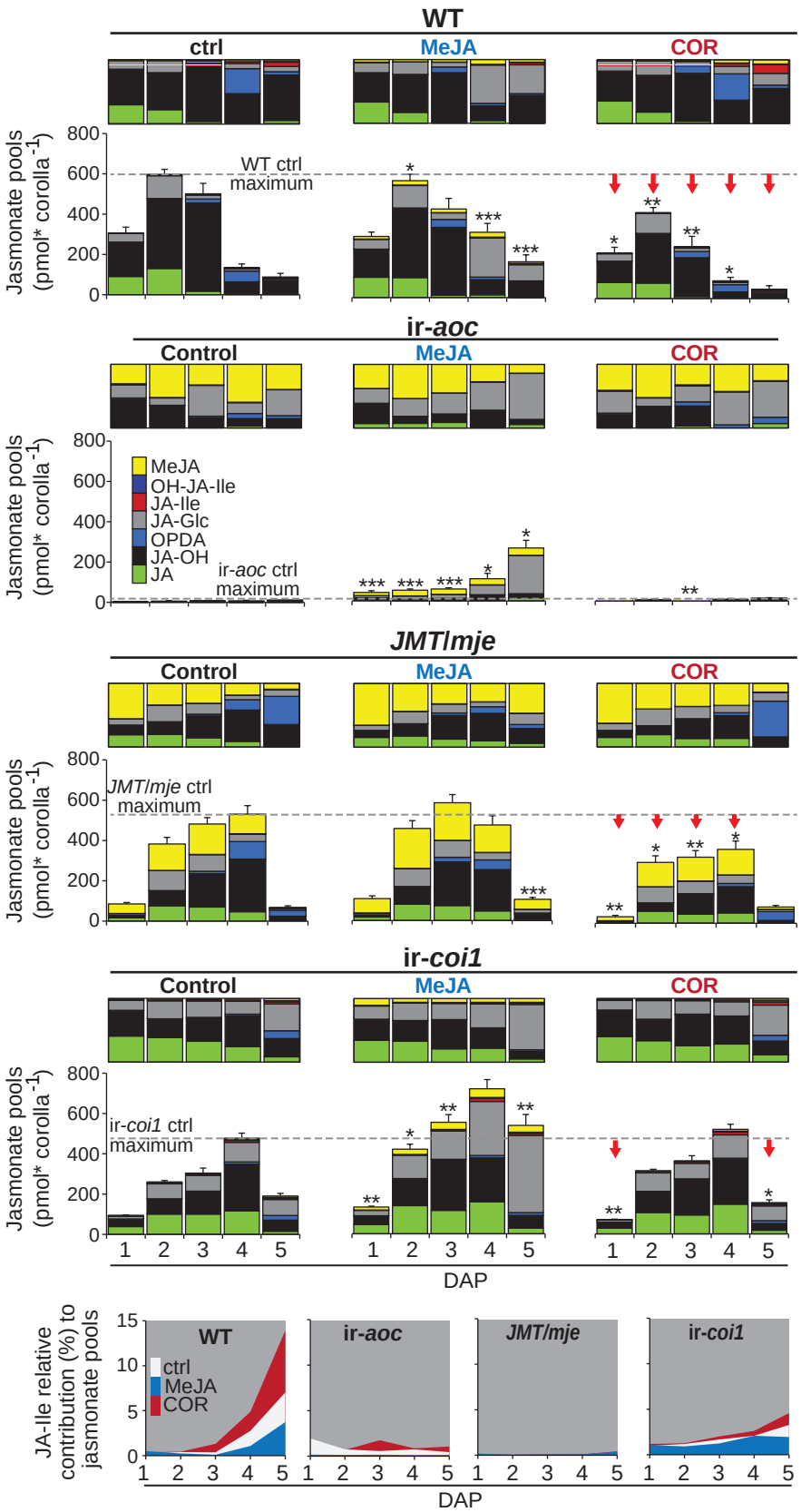

Supplemental Figure 6. COR application reveals a negative feedback effect of JA-Ile signaling on developmentally-regulated JAs pools of corollas. (**A**) Mean (+SE, *n* = 3) summed levels (lower panels) of the seven most abundant JAs (JA, OH-JA, OPDA, JA-Glc, JA-Ile, OH-JA-Ile and MeJA) as detected at the indicate time after protrusion (DAP; days after the corolla first protruded the sepals) in corolla tissues treated either with control, COR and MeJA solutions. JAs were quantified as described in the method section by HPLC-MS/MS analysis. Total JAs were expressed in pmol per corolla to take into account relative differences in genotype water contents. 100% stacked columns above jasmonate pools depict relative contribution of each JAs to the total jasmonate pools of wild type, ir-*aoc*, *JMT*/*mje* and ir-*coi1* corollas (normalized to 100%). Each replicate was obtained from 20+ pooled tissues of 3 plants. Grey dashed lines indicate the maximum levels measured in control corollas for each genotype. Asterisks indicate significant differences between control and MeJA or COR treated tissues of the same genotype and DAP (unpaired t-test; *, p <0.05, ** p <0.001, *** p <0.0001). (**B**) Relative contribution (%) of JA-Ile to jasmonate pools in corollas of control (white), COR (red) or MeJA (blue) treated plants. COR application increases the relative contribution of JA-Ile to the JAs pools.

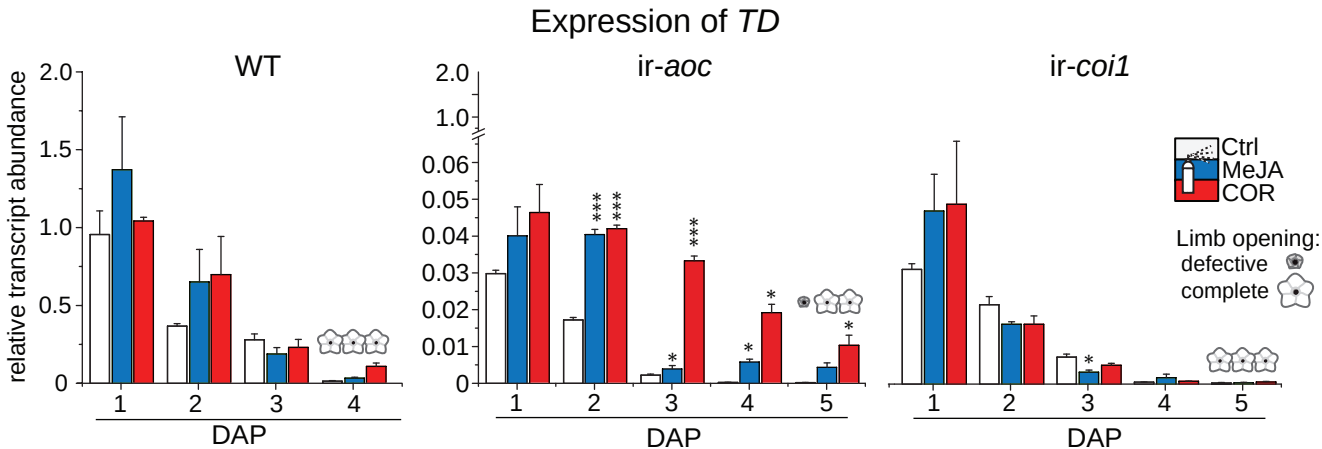

Supplemental Figure 7. Reduced *TD* transcript levels in JAs but not in COI1 deficient corollas are partly rescued by MeJA/COR application. Transcript abundance (relative to *ELONGATION-FACTOR 1ALPHA* (*EF1α*) gene expression) of *THREONINE DEAMINASE* (*TD*) in dissected corolla tissues of WT, ir-*aoc* and ir-*coi1* flowers at indicated day after protrusion (DAP; days after the corolla first protruded the sepals) and treatments (mean + SE, *n* = 3, each replicate was obtained from 20+ pooled tissues of 3 plants). MeJA/COR inhibit the developmental decline in AOC flowers more strongly than those in COI flowers. Asterisks represent significant differences between ctrl and treated tissues of the same genotype and DAP (unpaired t-test; *, $p < 0.05$; *** $p < 0.0001$).

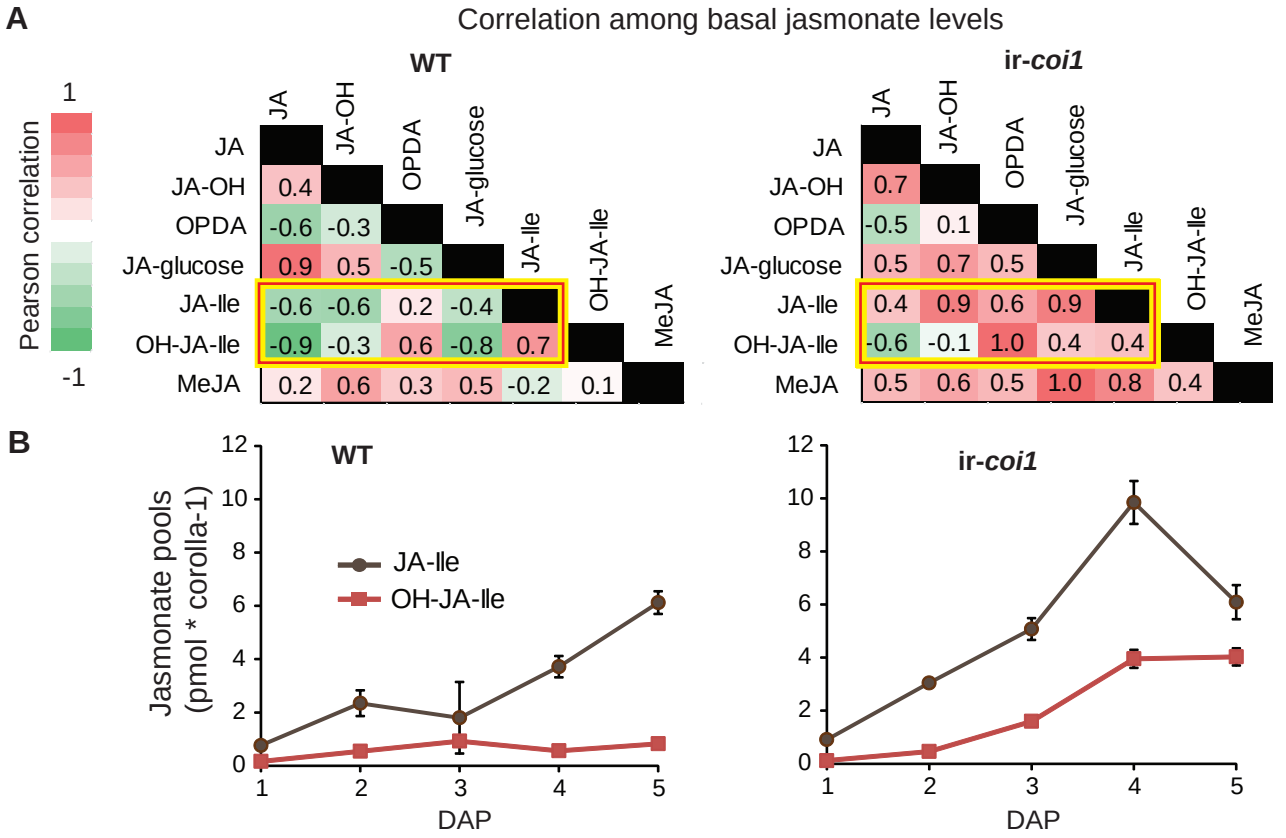

Supplemental Figure 8. Silencing *COI1* expression remodels developmentally regulated effects on JA-Ile accumulation. (A) Correlation matrices for basal JAs levels in untreated corollas of WT and ir-*coi1* plants. Expression vectors obtained for the developmental regulation of JAs levels in WT and ir-*coi1* corollas during the complete time line were used to compute intra-genotype pairwise Pearson correlation coefficients. Significant shifts in the correlation of JA-Ile and its main catabolite (OH-JA-Ile) with other JAs were observed when silencing *coi1*, which is clearly seen in increases in JA-Ile and OH-JA-Ile levels in ir-*coi1* corollas **(B)** Mean (± SE, *n* = 3, each replicate was obtained from 20+ pooled tissues of 3 plants) levels of JA-Ile and its main catabolite OH-JA-Ile in WT and ir-*coi1* corollas, highlighting the feedback control effect of COI1 on the homeostasis of JA-Ile. (DAP; days after the corolla first protruded the sepals).

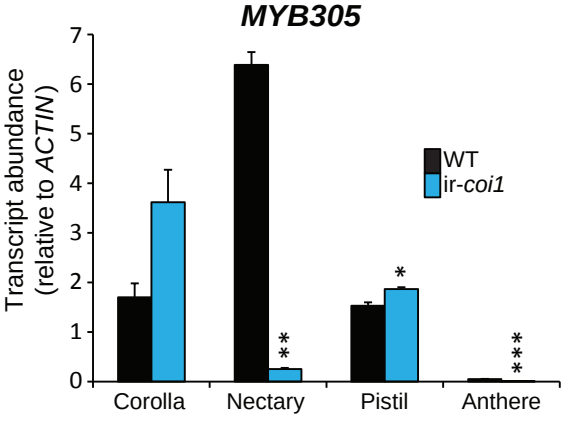

Supplemental Figure 9. Floral expression of *NaMYB305* primarily expressed in nectary tissues is impaired in COI1 deficient nectaries. Transcript abundance (relative to gene expression of *ACTIN*) of *MYB305* in individual floral tissues of WT and ir-*coi1* plants at the day before anthesis (mean + SE, $n = 3$, each replicate was obtained from 8+ pooled tissues of 4 plants). Asterisks represent significant differences between the same floral tissue of WT and ir-*coi1* (unpaired t-test; *, $p < 0.05$; **, $p < 0.001$; **, $p < 0.001$; *** $p < 0.0001$).

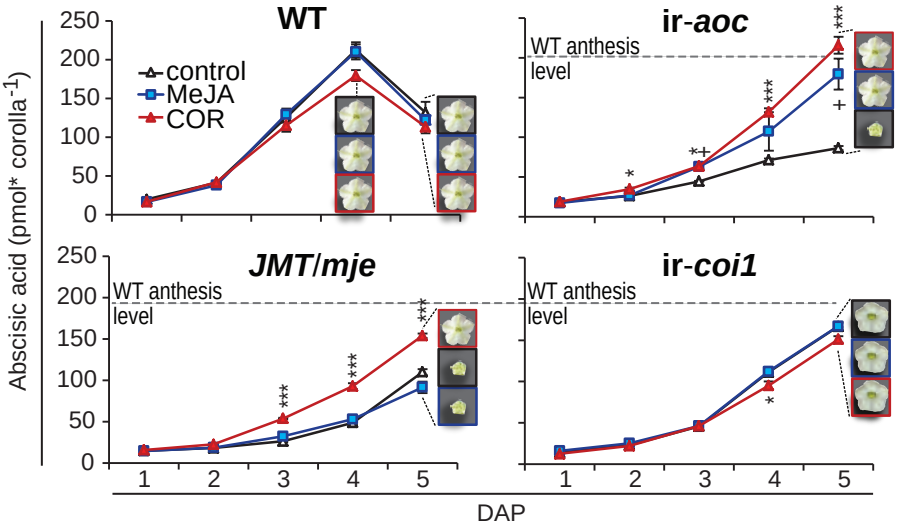

Supplemental Figure 10. Developmentally regulated abscisic acid (ABA) accumulation during corollas expansion involves COR/JA-Ile signaling. Levels of abscisic acid (ABA) as detected at the indicated day after corollas protruded sepals (DAP; days after the corolla first protruded the sepals) in dissected corolla tissues of wild type, ir-*aoc*, *JMT*/*mje* and ir-*coi1* flower buds (Mean ± SE, *n* = 3, each replicate was obtained from 20+ pooled tissues of 3 plants). Flower insets show opening state of flowers at anthesis. Grey dashed lines denote ABA levels of WT flowers at first night of anthesis. Asterisks (COR) and plus signs (MeJA) represent significant differences compared to control treated tissues of the same genotype. (unpaired t-test; */+ p <0.05, **/++ p <0.001, ***/+++ p <0.0001).

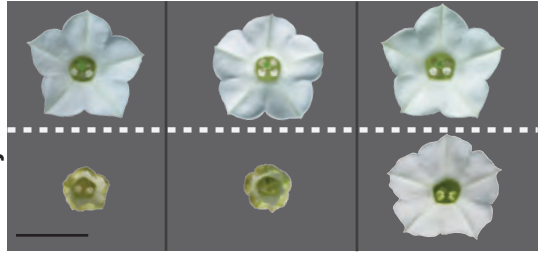

Supplemental Figure 11. ABA treatment does not restore corolla limb opening in JAs deficient flowers. WT and *JMT*/*mje* were treated every other day with 200 µM ABA as described in Ré et al., (2011), 1 µM coronatine (COR) or with a control solution. The opening of flower corollas was monitored one week after initial treatments. Scale bar, 10 mm.

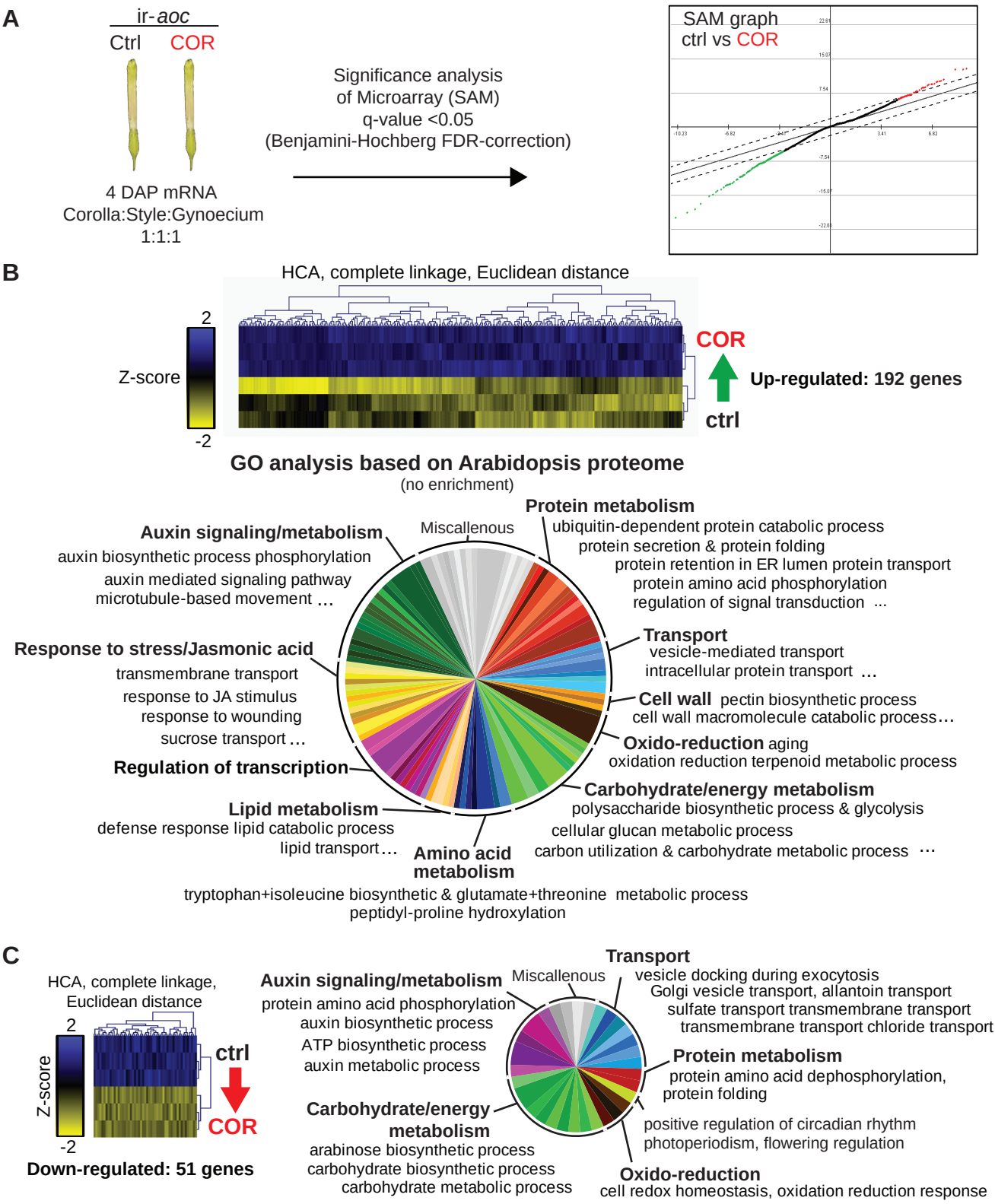

Supplemental Figure 12. Coronatine application on ir-*aoc* flowers activates transcriptomic changes in flower signaling, metabolic and developmental processes. (**A**) Experimental design for sample collection, microarray analysis and statistical analysis. Floral buds at 4 DAP (4 days after corolla protruded and appeared outside sepals) of ir-*aoc* - treated with ctrl (control) or 1µM COR (coronatine) solution - were dissected and 3 biological replicates of each tissue (complete corolla, style and gynoecium tissues) were collected. Individual replicates were obtained from 20+ flowers of each 2 plants. cDNA synthesized from extracted RNA pools were combined with an equal contribution of each tissue types. Microarray data (3 replicates obtained from 3 independently produced pools of cDNA) were 75-percentile normalized and analyzed using significance analysis of microarray (SAM, Benjamini-Hochberg FDR threshold of 5%) for differentially regulated genes between ctrl- and COR-treated flowers **(B,C)** Hierarchical clustering analysis (HCA) on differentially regulated genes and classification of encoded biological processes. Expression vectors for significantly up- (COR>ctrl) **(B)** and down-regulated **(C)** (ctrl>COR) genes were scaled using the Z-score function and aggregated by HCA using the Euclidean distance as clustering metric and the complete linkage method. Gene ontologies (GO) were attributed to differentially regulated probe sets according to best BlastX hits obtained with the Arabidopsis TAIR10 proteome for an e-value threshold of 1e-15. Pie charts depict relative proportions in up- and down-regulated biological processes. Biological processes were arbitrarily grouped as large process groups and examples of the main processes represented in each group are provided. For this Figure, unlike in **Figure S13**, biological process overrepresentation was not tested using hypergeometric tests.

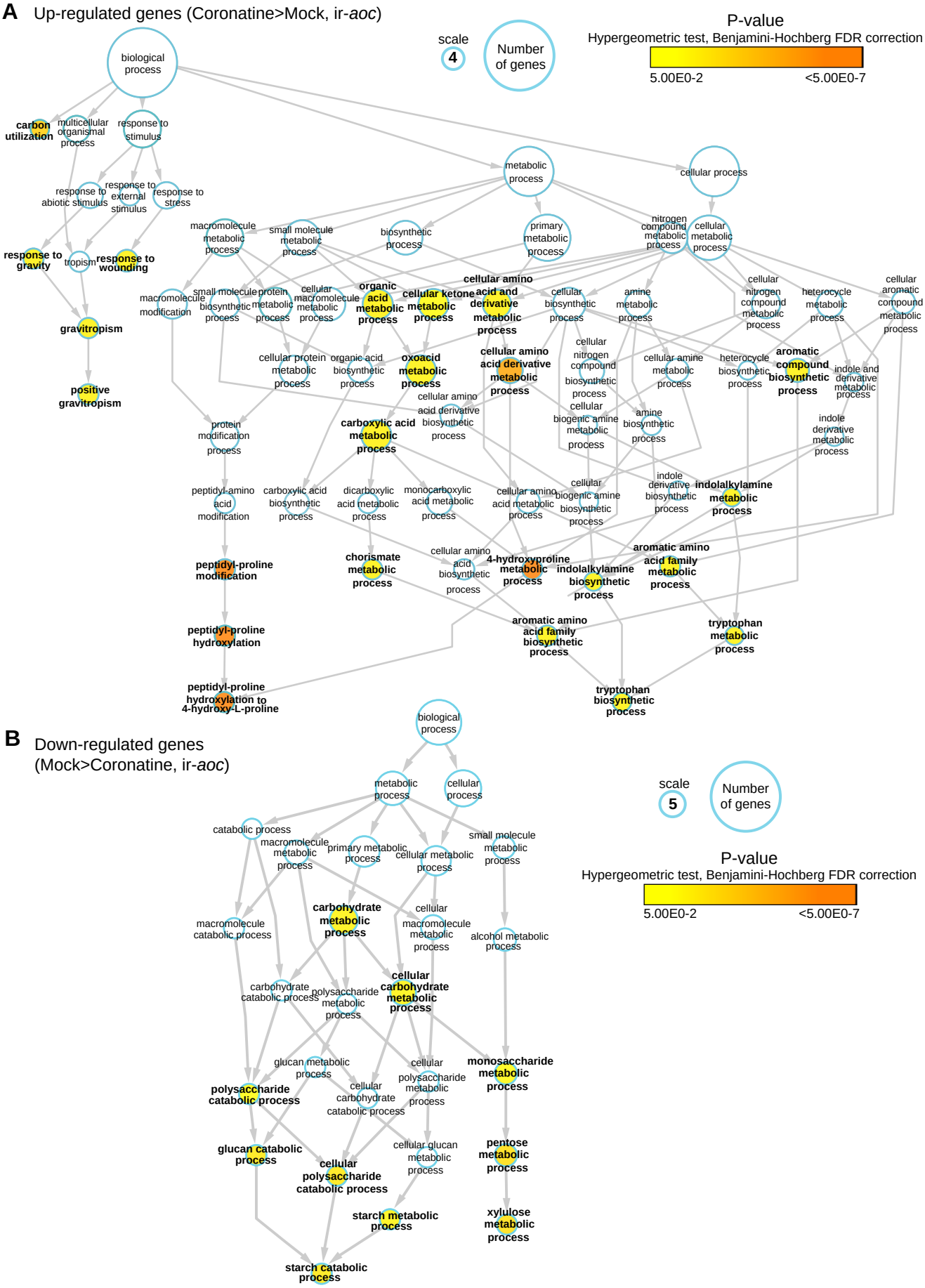

Supplemental Figure 13. BINGO analysis of biological process overrepresentation.

Overrepresentation analysis of ir-*aoc* flower genes significantly up- and down-regulated by the coronatine treatment identifies specific reconfigurations of primary and secondary metabolism transcriptional machineries. Up- and down-regulated genes by the coronatine treatment compared to the control solution and identified by SAM were independently analyzed using the BINGO plugin available for the network visualization software Cytoscape. GO terms were attributed according to best BlastX hits obtained with the Arabidopsis TAIR6 proteome for an e-value threshold of 1e-15. Overrepresentation for particular processes was assessed using hypergeometric tests with a Benjamini-Hochberg FDR correction threshold of 5% versus whole annotated genes. GO networks were constructed using the Cytoscape Hierarchical layout. Node size is proportional to the number of genes associated to a particular GO and node color denotes for the FDR-corrected P-value for a GO relative enrichment.

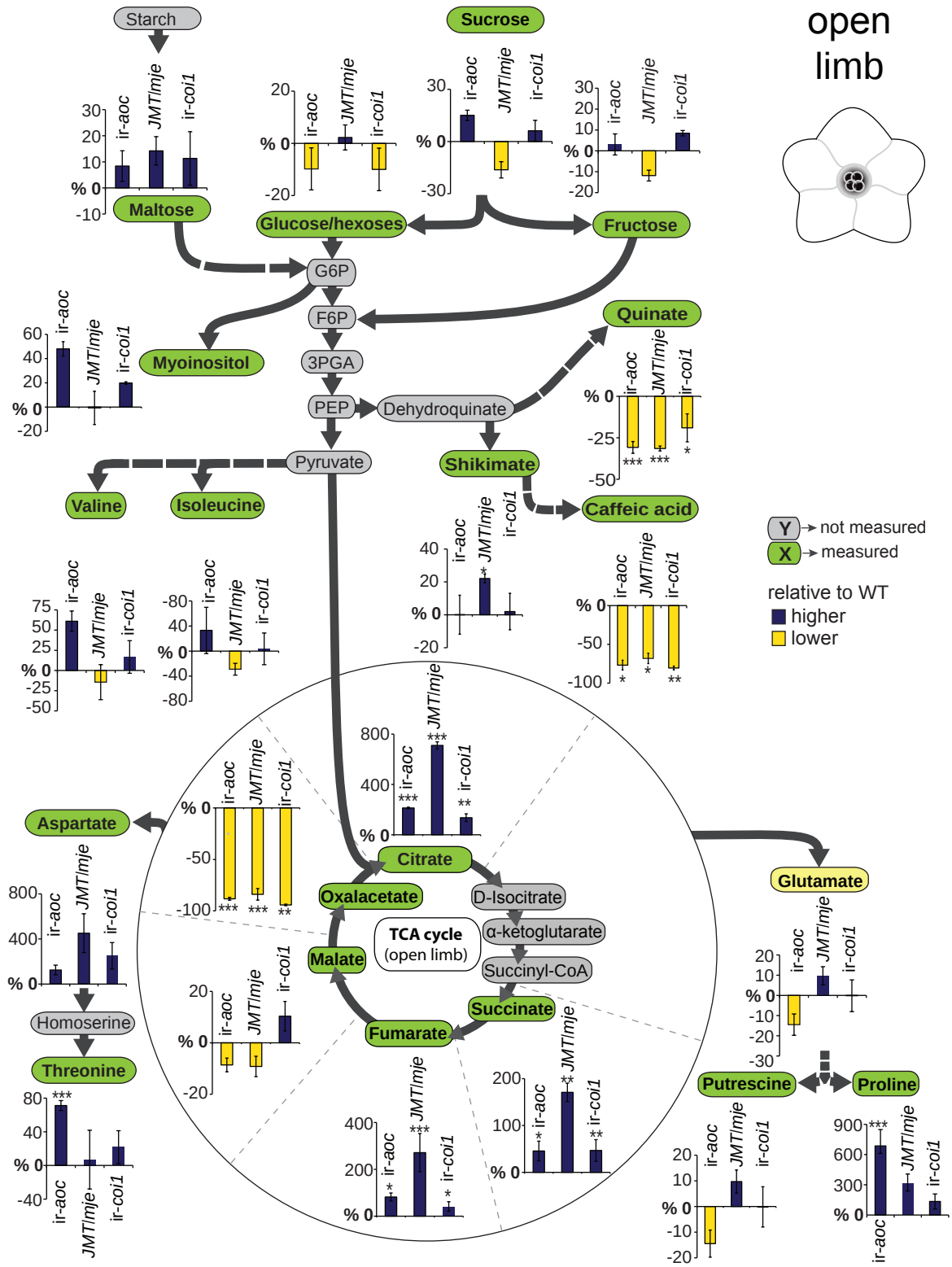

Supplemental Figure 14. Accumulation of carbohydrates and intermediates of energy metabolism in limbs at anthesis is altered in lines with alterations in the JAs-signaling cascade. Relative changes (%) in metabolite accumulation compared to WT as detected in corolla limbs at anthesis of control treated ir-*aoc*, *JMT*/*mje* and ir-*coi1* flowers. Blue bars indicate higher and yellow bars lower level than WT. Asterisks indicate significant differences compared to WT levels (mean + SE, *n* = 3, each replicate was obtained from 20+ pooled tissues of 3 plants). Glucose, combined glucose and hexoses; G6P, glucose 6-phosphate; F6P, fructose 6-phosphate; GADP, glyceraldehyde 3-phosphate; PEP, phosphoenolpyruvate. Derivatized metabolic extracts were analyzed by GCxGC-TOF-MS as described in Gaquerel et al. (2009). Asterisks denote significant differences between limb tissues of WT and corollas tissues of transgenic (unpaired t-test; * p <0.05, ** p <0.001, *** p <0.0001).

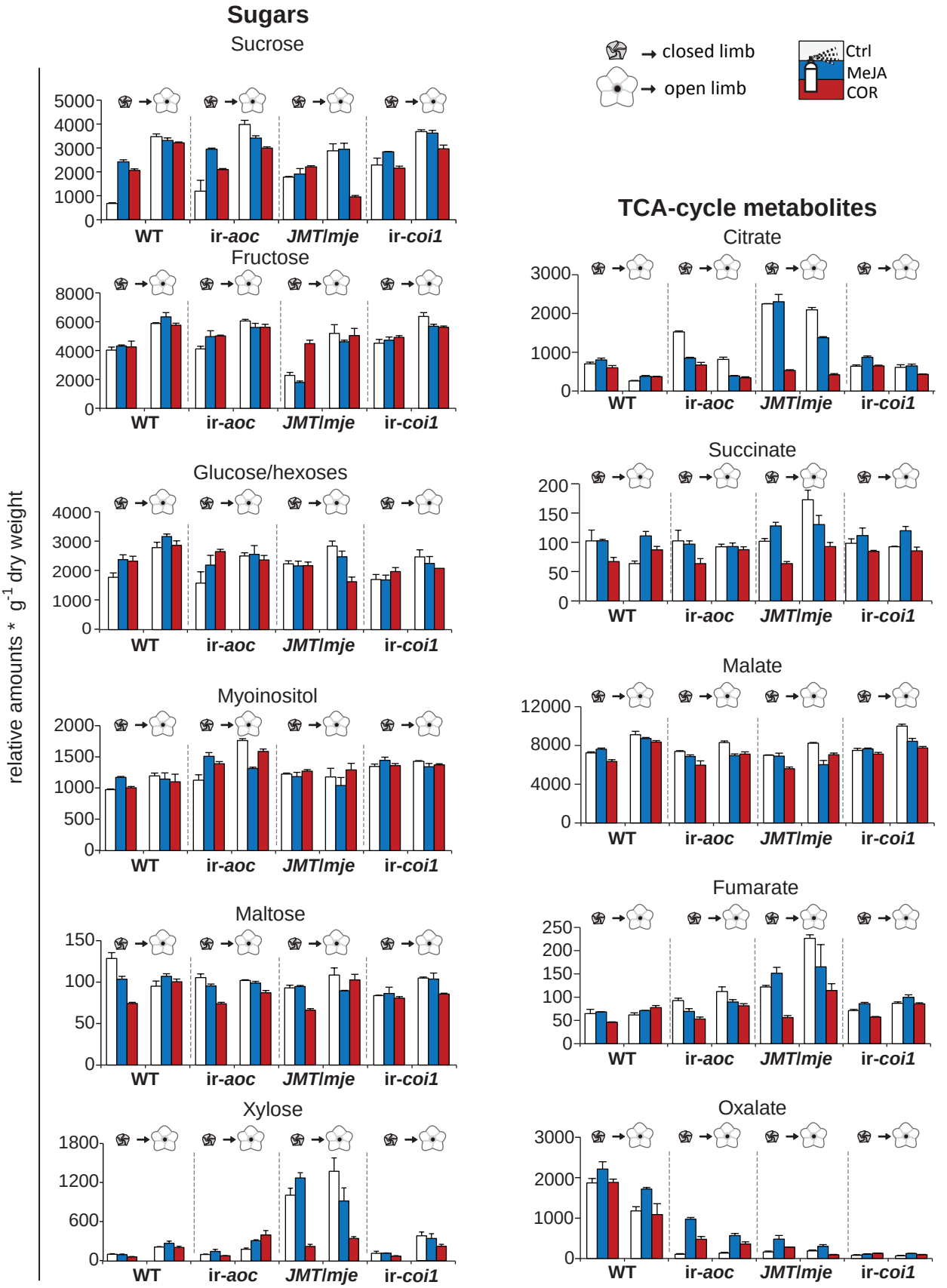

Supplemental Figure 15. Developmental changes in carbohydrate composition and accumulation of intermediates of the TCA cycle during anthesis are regulated via JAs signaling. Metabolite accumulation was monitored in closed and open corolla limbs of WT, ir-*aoc*, *JMT*/*mje* and ir-*coi1* flowers after control (Ctrl/white), methyl jasmonate (MeJA/blue) and coronatine (COR/red) treatment (mean + SE, *n* = 3, each replicate was obtained from 20+ pooled tissues of 3 plants). Glucose, combined glucose and hexoses. Samples were analyzed by GCxGC-TOF-MS as described in Gaquerel et al. (2009).

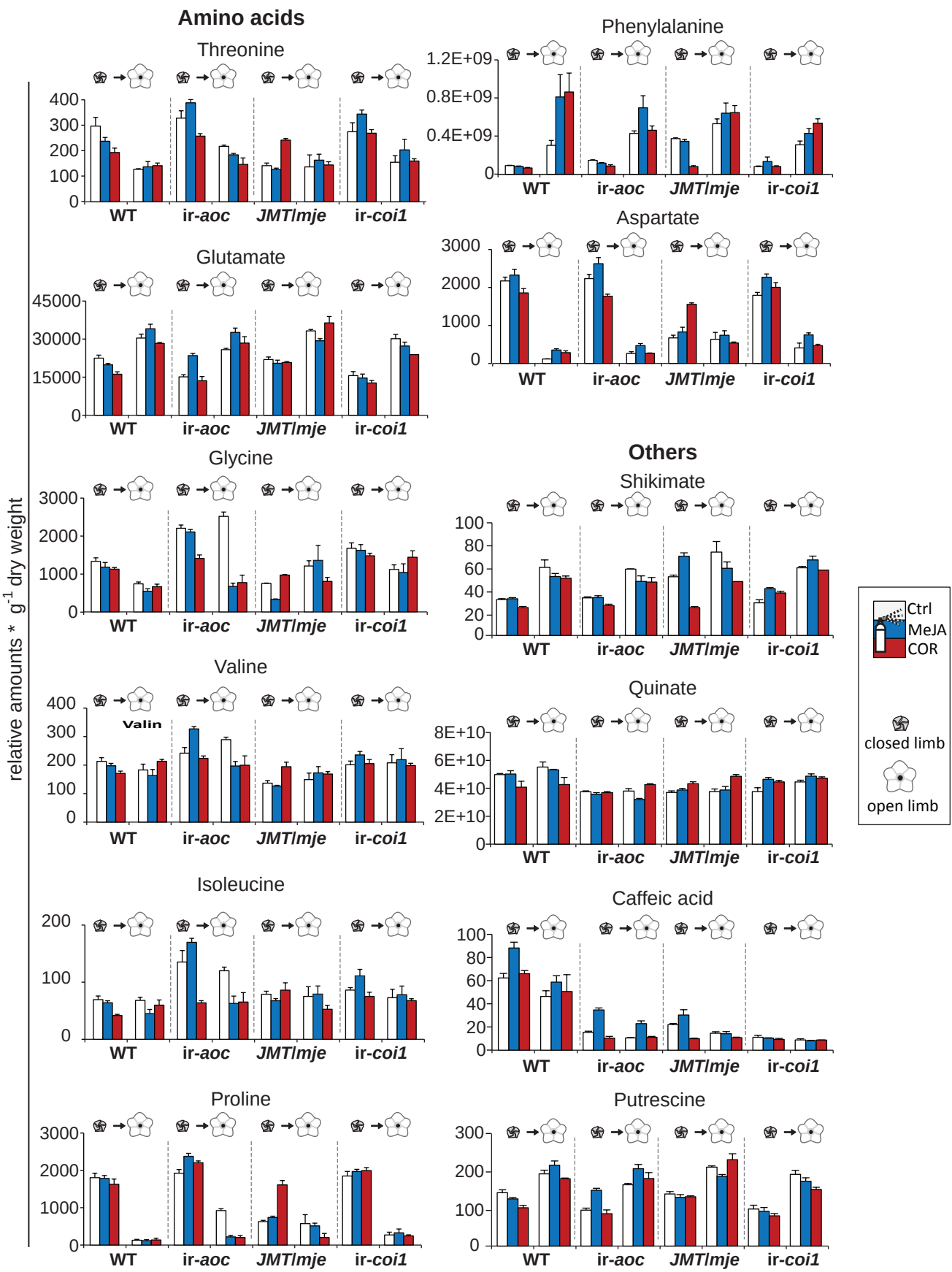

Supplemental Figure 16. Limb accumulation of some amino acids and other metabolites is compromised by JAs deficiency and can be rescued by MeJA or COR applications.
Metabolite accumulation was monitored in closed and open corolla limbs of WT, ir-*aoc*, *JMT*/*mje* and ir-*coi1* flowers after control (Ctrl/white), methyl jasmonate (MeJA/blue) and Coronatine (COR/red) treatment (mean + SE, *n* = 3, each replicate was obtained from 20+ pooled tissues of 3 plants). Samples were analyzed by GCxGC-TOF-MS as described in Gaquerel et al.(2009).

Supplemental Table 1. Sequences of gene-specific primers used for RT-qPCR.

Gene	Forward Primer	Reverse primer
ACTIN	5´-GGTCGTACCACCGGTATTGTG-3´	5´-GTCAAGACGGAGAATGGCATG-3´
AOS	5´-GACGGCAAGAGTTTTCCCAC-3´	5´-TAACCGCCGGTGAGTTCAGT-3´
BAM	5´-ACACAGATCAGTGGGGAAGG -3´	5´-ACAATGGTGTCCCCTAGCAG-3´
CHAL1	5´-TCATTTGGATAGTATGGTCGGG-3´	5´-ACCGTTGATAGCGCCATCGC-3´
COI1	5´-CAGGGCATCTTCAGCTGGTC-3´	5´- CGGGATGCTCAGCAACGA-3´
EF1	5´-CCACACTTCCCACATTGCTGTCA-3´	5´-CGCATGTCCCTCACAG-3´
JAZd	5´-GAGATTGTAGATTCCGGCAAGGTCA-3´	5´-TTCTCAGCTGAATCACCTGA-3´
MYB305	5´-ATGCTAAGTGGGGAAACAG-3´	5´-GCAATTGCATGGACCAGA-3´
NEC1	5´-TGCTGTTTTTGCCGCTCCTT-3´	5´-ACCACATCGTGGCACAGAGAGT-3´
OPR	5´-ATGCCAGATGGAACTCATGCTATTT-3´	5´-TATCAAACTTGCCAAGATTCTGAGC-3´
TD	5´-TAAGGCATTTGATGGGAGGC-3´	5´-TAAGGCATTTGATGGGAGGC-3´